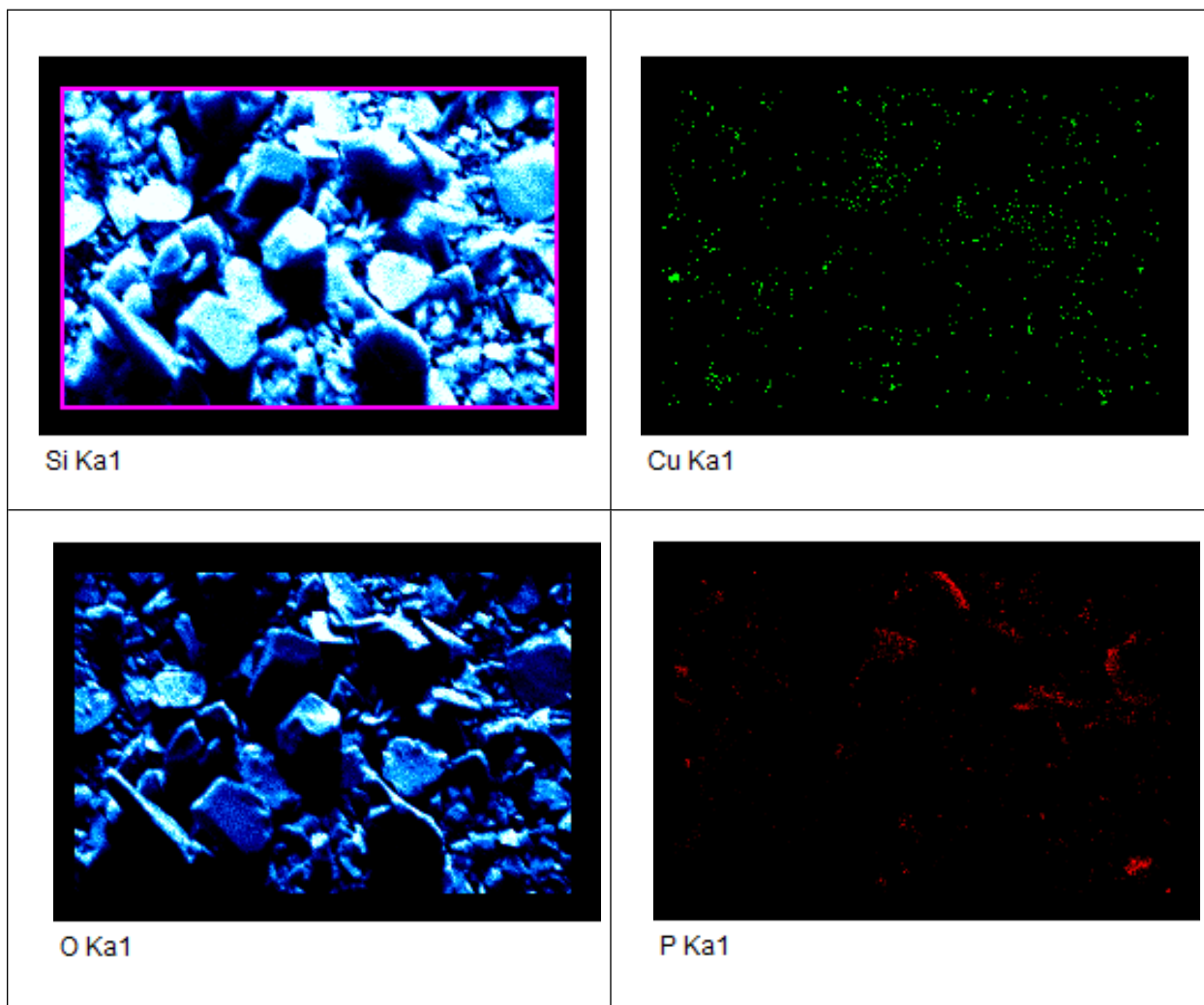
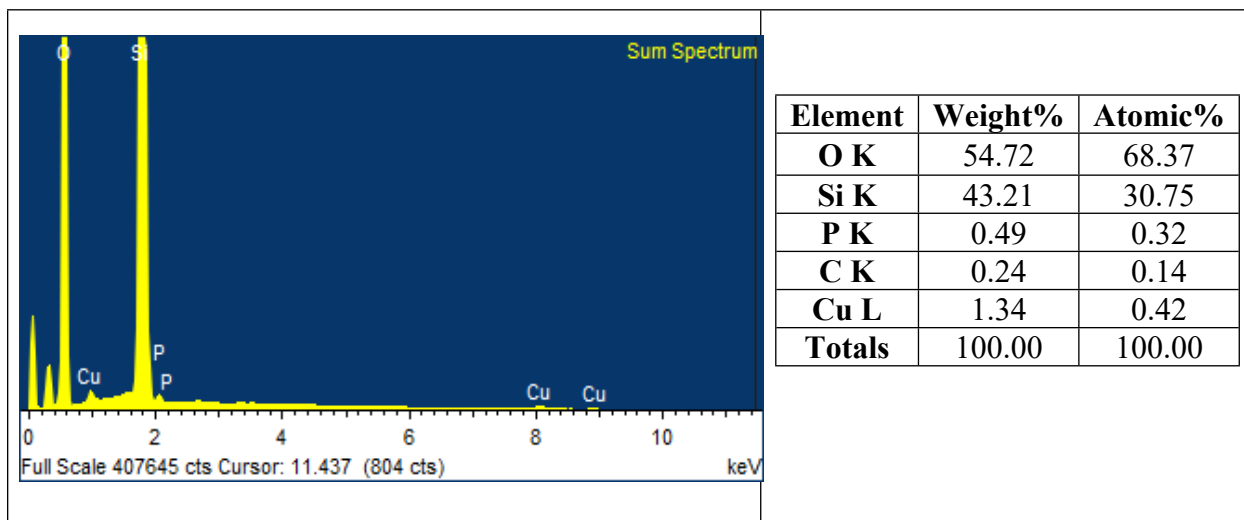


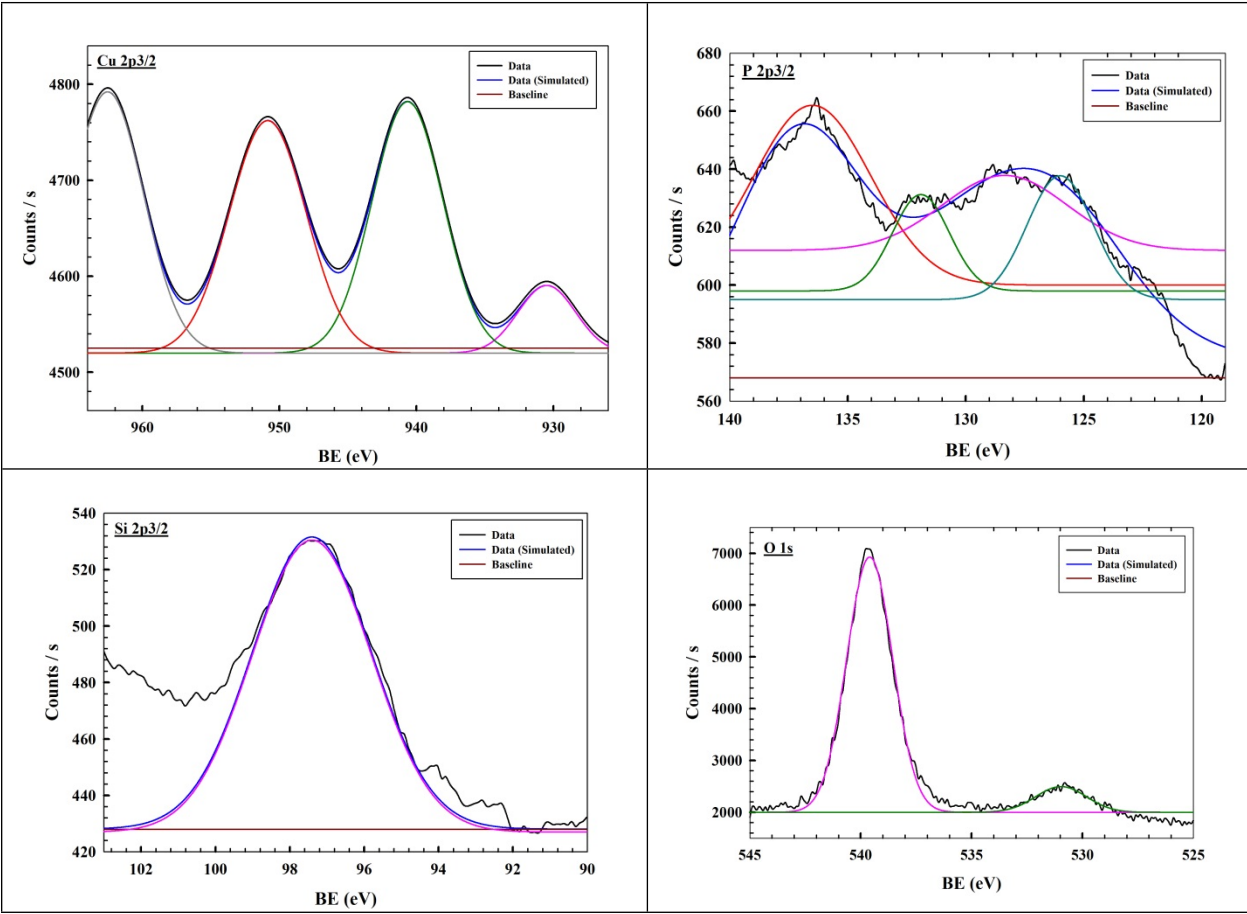
Supplements



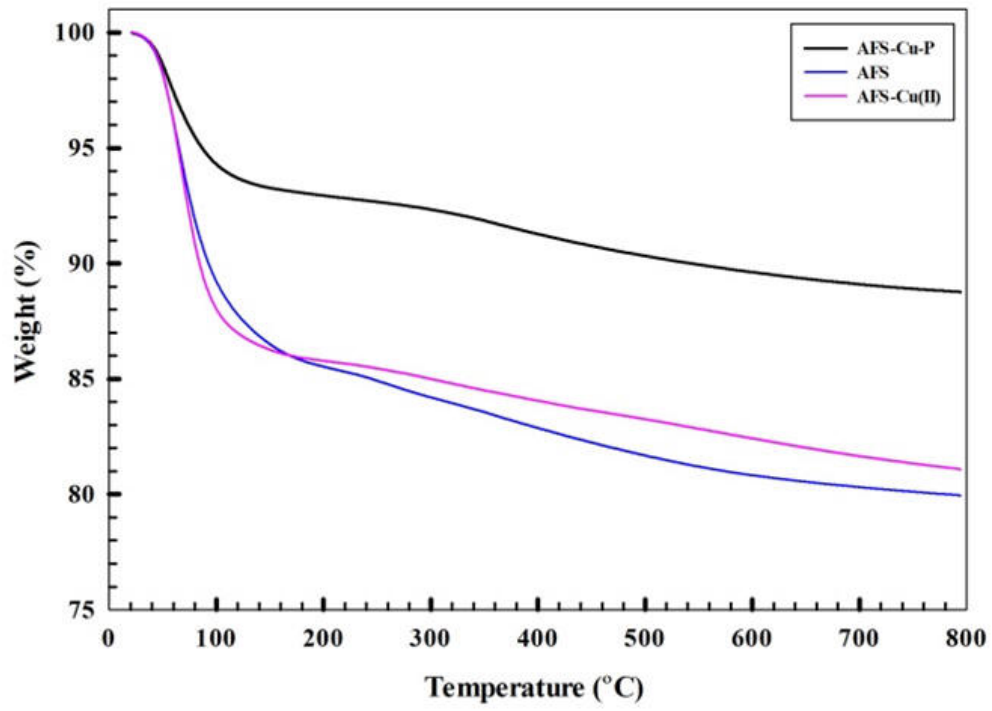
Supplement 1a. Surface elemental mapping of the AFS-Cu-P catalyst showing Si, O, Cu and P elements



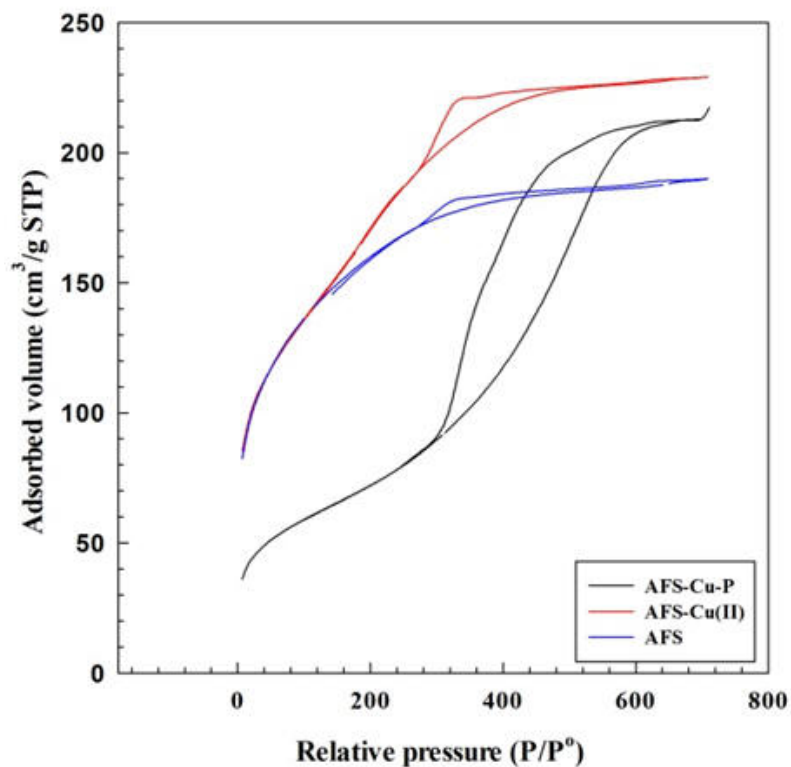
Supplement 1b. EDS data and elements percentage of the AFS-Cu-P catalyst components



Supplement 2. XPS of copper, phosphorus, silicon and oxygen in the AFS-Cu-P catalyst



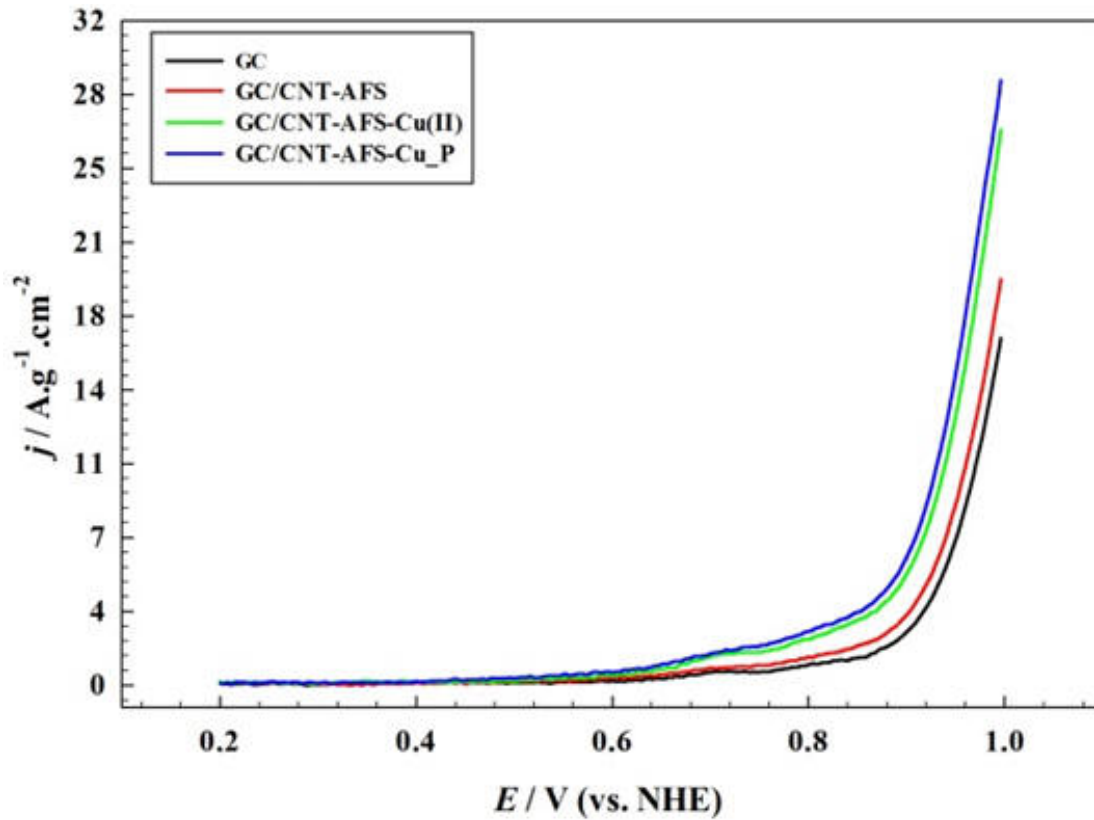
Supplement 3. TGA profile of the as-prepared AFS-Cu-P; Comparison with AFS-Cu(II) and AFS



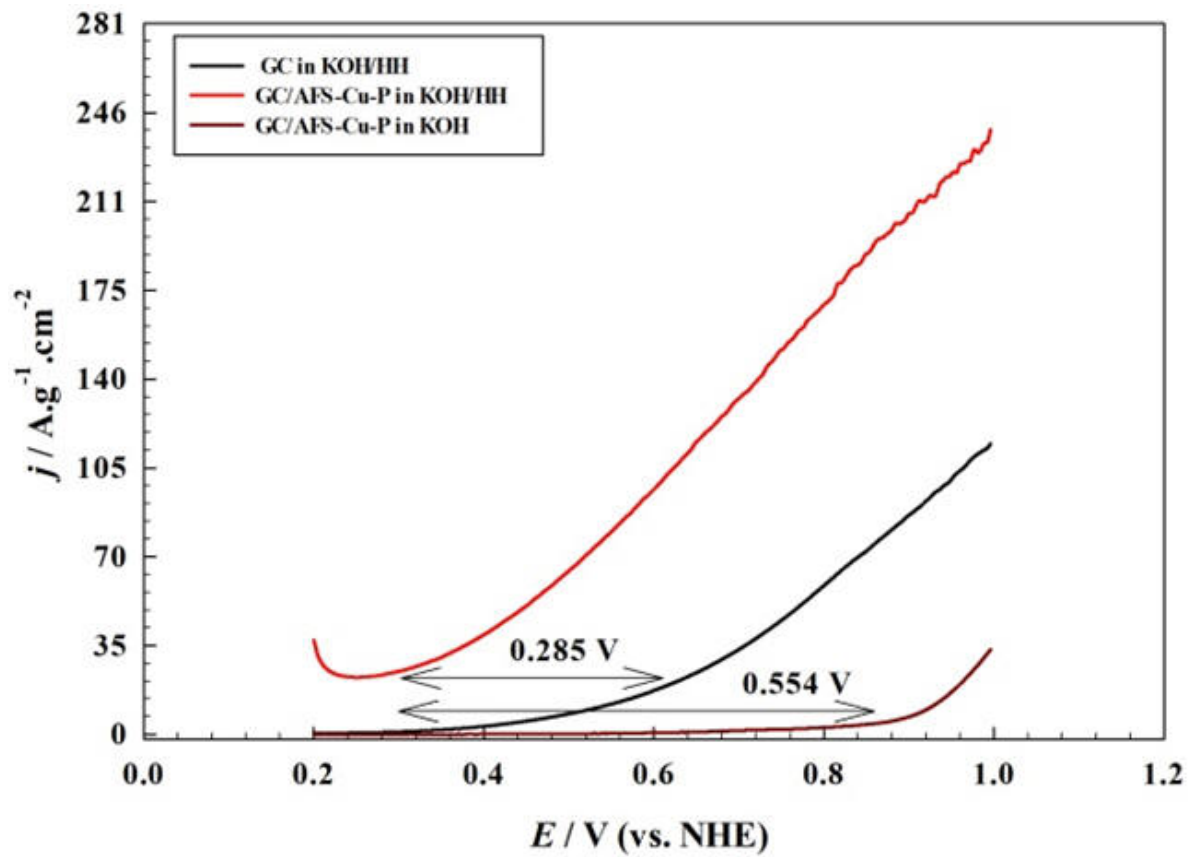
Supplement 4a. BET isotherm for the as-prepared AFS-Cu-P catalyst and the AFS-Cu(II)

Supplement 4b. Summary of the BET results for AFS-Cu-P catalyst, AFS-Cu(II), and AFS

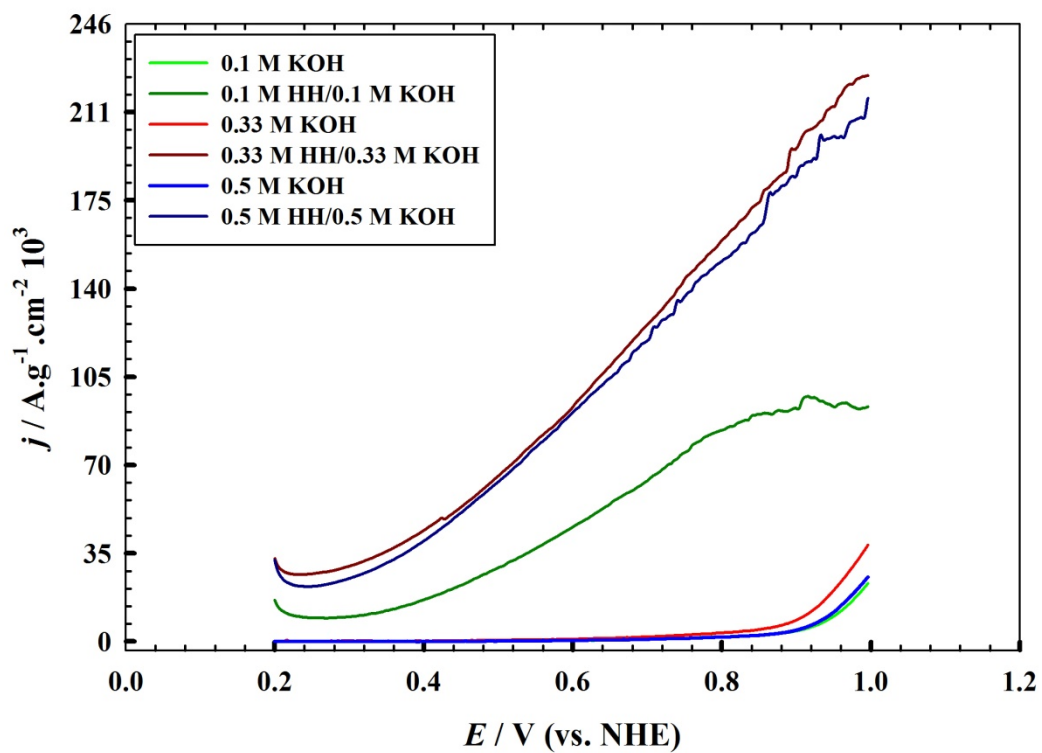
	AFS	AFS-Cu(II)	AFS@100 Phos-Cu
BET Surface Area (m²/g)	525.32	546.15	232.38
Langmuir Surface Area (m²/g)	769.18	808.38	341.53
Pore Volume cm³/g	0.29399	0.35393	0.32922



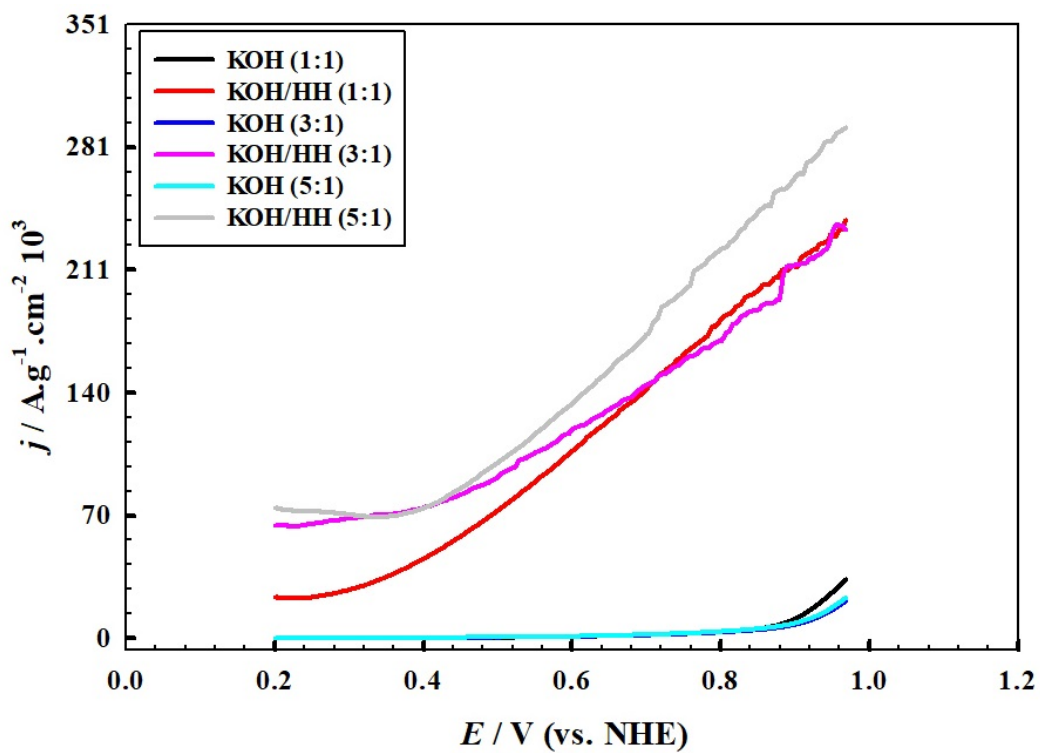
Supplement 5. Comparison of the linear sweep voltammograms of the GC/CNT-AFS-Cu-P, GC/CNT-AFS-Cu(II) and GC/CNT-AFS electrodes in 1.0 M KOH



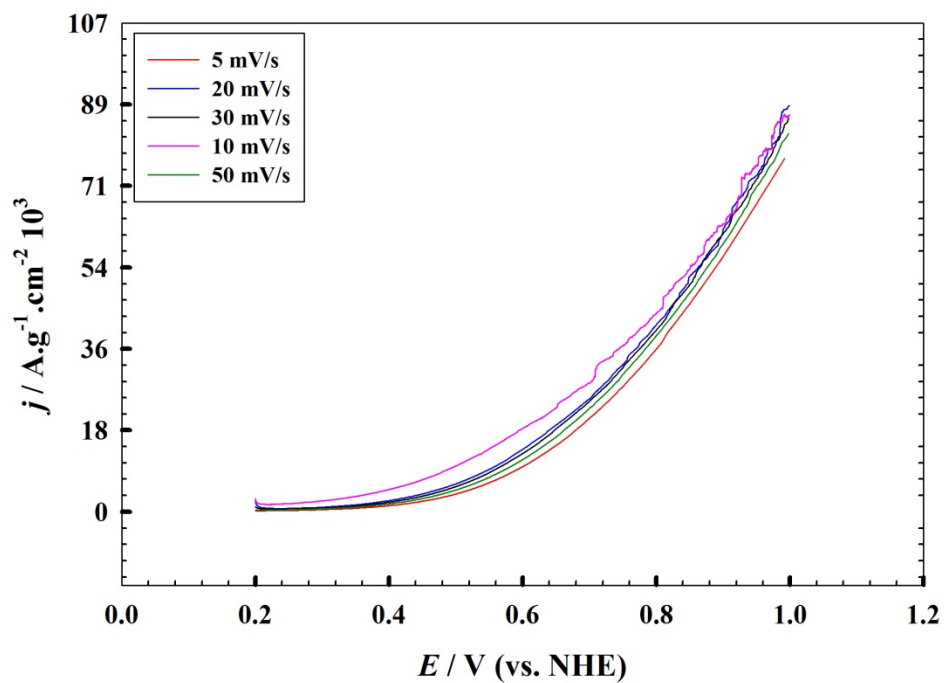
Supplement 6. Comparison of the linear sweep voltammograms of the GC/CNT-AFS-Cu-P electrode in presence and absence of hydrazine with GC in presence of hydrazine/1.0 M KOH



Supplement 7. Effect of hydrazine concentration on the oxygen evolution reaction at the GC/CNT-AFS-Cu-P electrode; the concentration ratio of hydrazine to KOH was kept constant. The scan rate is $10 \text{ mV}\cdot\text{s}^{-1}$



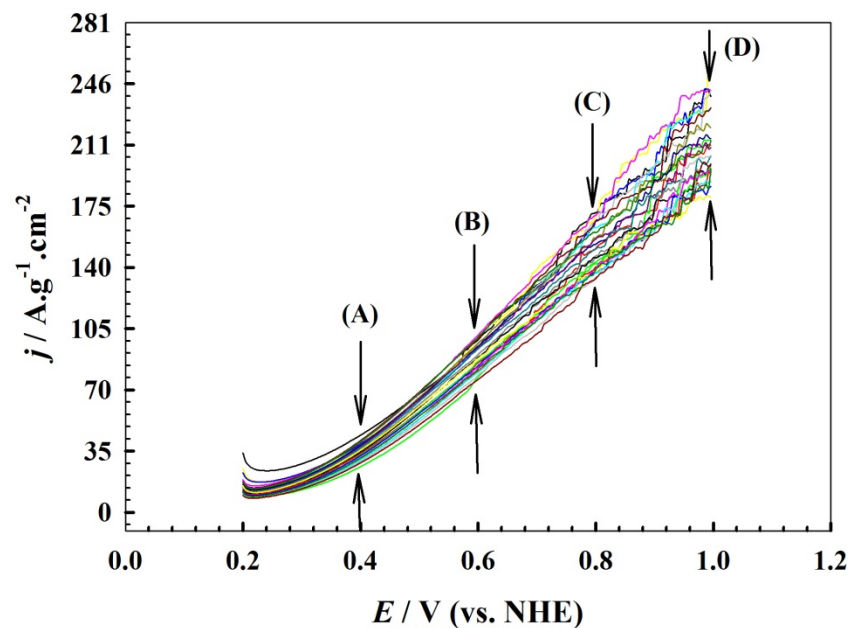
Supplement 8. Effect of KOH concentration on the oxygen evolution reaction at the GC/CNT-AFS-Cu-P electrode. The scan rate is $10 \text{ mV}\cdot\text{s}^{-1}$.



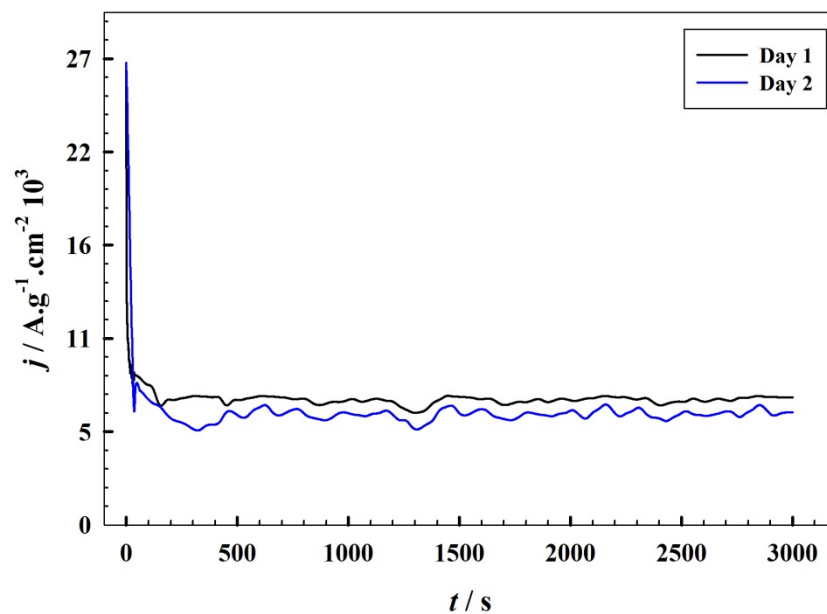
Supplement 9. Effect of varying the scan rate on the linear sweep voltammograms behavior of the electrode GC/CNT-AFS-Cu-P in 0.33 M hydrazine/ 1.0 M KOH.

Electrode Material/Molecular Species	Molecular Species Oxidation Overpotential	OER Overpotential	Current Density/ Specific Current	Overpotential
Co _{0.52} Cu _{0.48} /Cu@S-C Hydrazine[89]	118 mV	1.3 V	10, 100 and 200 mA.cm ⁻²	36, 210 and 282 mV
D/Ni-Cu-Se/NF Urea[90]	1.335 V	1.395 V	10 mA cm ⁻²	1.335 V
RuCo/C Hydrazine[91]	76.8 mV	-	100 mA·cm ⁻²	215.4 mV
Pd/NiCo ₂ O ₄ Hydrazine[92]	6 mV	-	10 and 100 mA.cm ⁻²	0.35 V and 0.94 V
Co PANI/C Hydrazine[93]	0.34 V	0.906 V	-	-
Mn-doped Ni ₂ P Hydrazine[94]	55 mV	0.5 V	10 mA.cm ²	55 mV
Cu ₂ O-S-Co-CoFe Hydrazine[95]	0.343 V	307 mV	20 mA.cm ⁻²	0.36 V
Cu-CoFe/Co/NC[96]	281 mV	0.87 V	10 mA.cm ²	281 mV
RuNi Hydrazine[97]	65 mV	-	10 mA.cm ⁻² and 100 mA.cm ⁻²	57.8 mV and 327 mV
CNT-AFS-Cu-P Hydrazine (this work)	186 mV	298 mV	32 A.g ⁻¹ .cm ⁻²	298 mV

Supplement 10. Comparison of the performance of the present catalyst to copper- and others-based catalysts with some figures of merit.



Supplement 11a. Repeated linear sweep voltammograms (LSVs) of the GC/ CNT-AFS-Cu-P electrode in 0.50 M KOH in the presence of 0.33 M hydrazine with a scan rate of 10 mV.s⁻¹.



Supplement 11b. Chronoamperometry of the GC/ CNT-AFS-Cu-P electrode exposed constant applied potential of 0.05 V in 0.33 M hydrazine/1.0 M KOH for an extended time of one hour.